


A. KOSTEREV
G. WYSOCKI
Y. BAKHIRKIN
S. SO
R. LEWICKI
M. FRASER
F. TITTEL 
R.F. CURL

Application of quantum cascade lasers to trace gas analysis

Rice Quantum Institute, Rice University, 6100 Main St., Houston, TX 77005, USA

Received: 18 September 2007/
Published online: 8 December 2007 • © Springer-Verlag 2007

ABSTRACT Quantum cascade (QC) lasers are virtually ideal mid-infrared sources for trace gas monitoring. They can be fabricated to operate at any of a very wide range of wavelengths from $\sim 3 \mu\text{m}$ to $\sim 24 \mu\text{m}$. Seizing the opportunity presented by mid-infrared QC lasers, several groups world-wide are actively applying them to trace gas sensing. Real world applications include environmental monitoring, industrial process control and biomedical diagnostics. In our laboratory we have explored the use of several methods for carrying out absorption spectroscopy with these sources, which include multipass absorption spectroscopy, cavity ring down spectroscopy (CRDS), integrated cavity output spectroscopy (ICOS), and quartz-enhanced photoacoustic spectroscopy (QEPAS).

PACS 42.62.Fi; 42.62.Be; 07.88.+y; 33.20.Ea

1 Introduction

Infrared laser absorption spectroscopy (LAS) is an extremely effective tool for the detection and quantification of molecular trace gases with demonstrated detection sensitivities ranging from ppmv and ppbv, to even pptv levels depending on the specific gas species and the detection method employed [1, 2]. These high sensitivities are obtained using fundamental vibrational molecular absorption bands in the mid-infrared (wavelength range from 3 to 24 μm).

Absorption spectra in the mid-IR of several small molecules of potential interest for trace gas monitoring are depicted in Fig. 1. The upper panel shows absorption spectra in the atmospheric window between the bending fundamental of water centered at around $\sim 1600 \text{ cm}^{-1}$ and the water OH stretches starting above 3200 cm^{-1} . The lower panel shows absorption spectra in the atmospheric window below the water bending fundamental. The logarithmic ordinate scales are the integrated intensities of the lines on a per-molecule basis. Since the peak absorption is the integrated absorption divided by the line width, the Doppler limited peak absorptions will be

correspondingly higher relative to the integrated absorption number at lower frequencies as the Doppler width is proportional to frequency.

Because the vibrational fundamentals have the largest absorption coefficients, they are the most suitable for high sensitivity trace gas detection of small and large molecules provided appropriate tunable laser sources are available. For real world trace gas monitoring applications, these laser sources should be compact and continuous wave (cw), efficient, and operate at near room-temperature and be reliable for long periods of time.

Existing tunable cw lasers operating in the mid-infrared include cw lead salt diode lasers, coherent sources based on difference frequency generation (DFG), optical parametric oscillators (OPOs), tunable solid state lasers, quantum and interband cascade lasers. Sensors based upon lead salt diode lasers are typically large in size and require cooling to temperatures of less than 90 K. DFG sources (especially periodically poled lithium niobate based bulk and waveguide) have been shown to be robust and compact [3–5] enough for desktop-type applications but are typically limited to wavelengths shorter than 5 μm and have limited mid-infrared output power. CW OPOs offer significant output power, however they are still too large and costly for field deployable sensors.

As the result of recent advances in the technologies of their fabrication, quantum cascade (QC) and interband cascade (IC) lasers have become attractive sources for ultra sensitive and highly selective, mid-infrared absorption spectroscopy [6]. At present, the most useful mid-infrared QC laser sources are based on type-I intersubband transitions in InGaAs/InAlAs heterostructures. These thermo-electrically cooled (TEC) QC lasers possess the narrow linewidths and high powers (tens to hundreds of mW in single frequency operation) that make these devices highly effective in laser absorption spectroscopy. These characteristics permit the creation of compact, robust trace gas sensors. Their relatively high power makes possible the use of a variety of spectroscopic detection techniques such as long open path laser absorption spectroscopy (including remote sensing techniques such as light detection and ranging, LIDAR or differential absorption LIDAR), cavity ringdown and integrated cavity out-

 Fax: +1-713-348-5686, E-mail: fkt@rice.edu

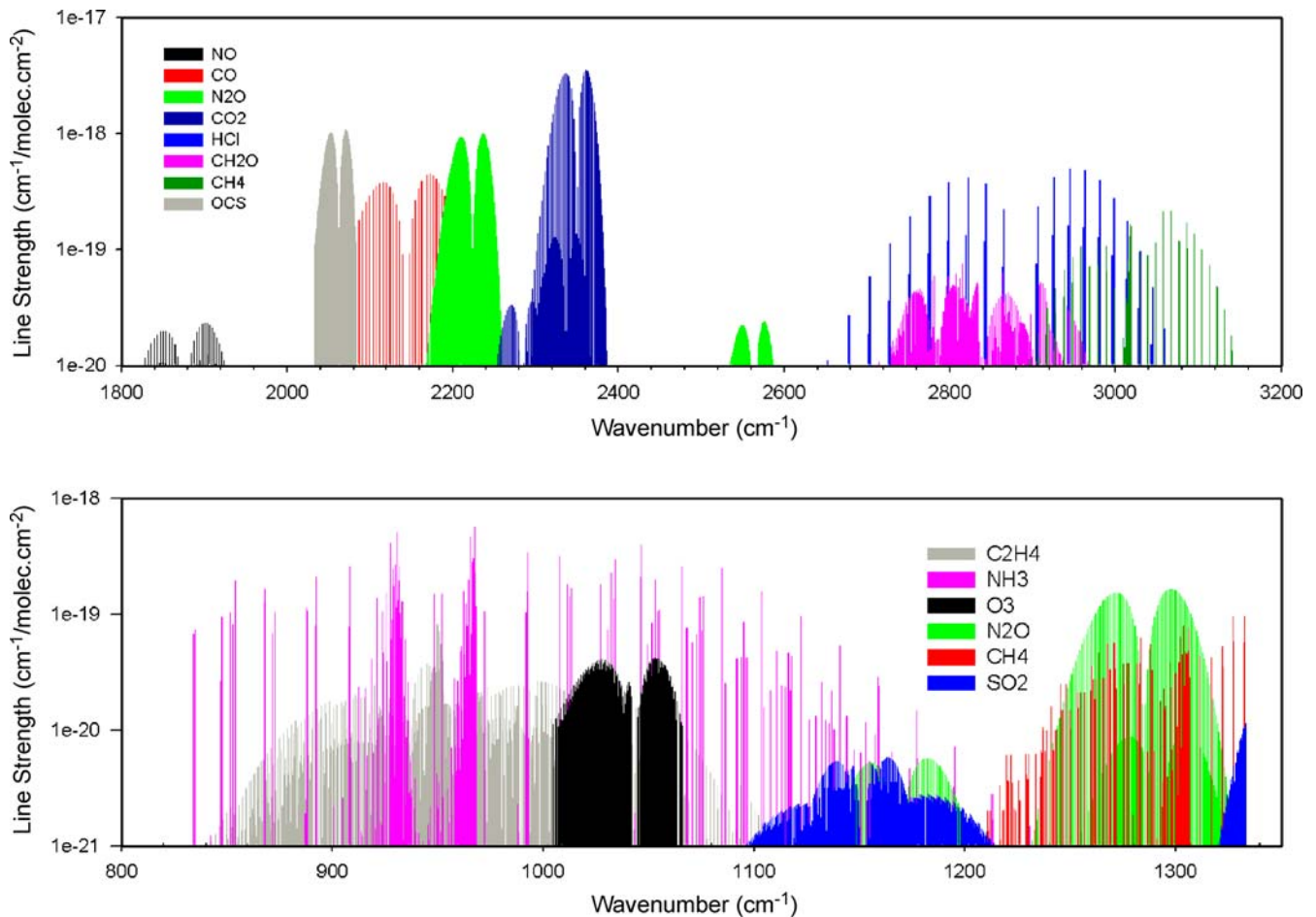


FIGURE 1 HITRAN simulation of absorption spectra

put spectroscopies, photoacoustic spectroscopy and evanescent field monitoring using fibers and waveguides. Seizing the opportunity presented by the availability of mid-IR QC lasers, several groups worldwide are actively applying them to trace gas sensing [7–13].

In our laboratory we have explored the use of several methods for carrying out absorption spectroscopy with these sources: multipass absorption spectroscopy [14], cavity ring down spectroscopy [15], integrated cavity output spectroscopy (ICOS) [16], and quartz-enhanced photoacoustic spectroscopy (QEPAS) [17]. Practical applications from our laboratory include: monitoring of formaldehyde in the Houston atmosphere [18], monitoring of NO in human breath [19], monitoring NH₃ in a NASA bioreactor [20] and detection of traces of CO in propylene [21]. There is a website [22] with a complete listing of publications on trace gas sensing at Rice.

In this paper we will first discuss the properties of quantum cascade lasers including widely tunable QCL sources, which are expected to be of great value to high resolution spectroscopy and gas phase radical chemical kinetics. This will be followed by a discussion of the requirements of trace gas sensing and the various methods for improving sensitivity including our QEPAS technology. Then some applications of QC lasers to trace gas sensing will be described. Finally we look to the future to discuss networks of sensors.

2 Properties of quantum cascade lasers

High optical power and single frequency operation with good spectral purity and wide tunability of the laser source are the most critical characteristics for chemical trace gas sensing using spectroscopic techniques. A simple QC laser with its cavity formed by the Fresnel reflections at its ends typically operates simultaneously in multiple longitudinal modes. This behavior has a straightforward explanation. In a linear cavity a mode is a standing wave. At the nodes of a standing wave, the mode power is zero and therefore inversion depletion at these locations by stimulated emission from the mode is small. However, another mode under the gain profile may have an antinode at these locations and consequently be over threshold. Thus the laser operates in several modes.

Single frequency operation is usually achieved by introducing a distributed feedback (DFB) structure into the QCL active region in order to favor a particular mode. Although state-of-the-art DFB QCLs show high performance and reliability, actually obtaining a laser with the optimum emission wavelength for a desired target analyte is technically challenging, because the range of wavelength tuning is strongly limited by the wavelength tuning range of the embedded DFB structure. Typically the maximum tuning range of DFB-QCLs achieved by changing the laser injection current is

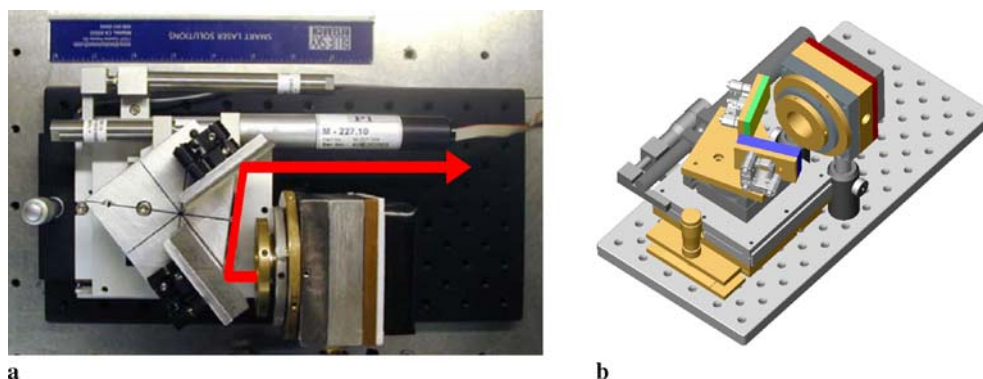


FIGURE 2 (a) A photograph and (b) a 3D mechanical model of a compact tunable external grating cavity quantum cascade laser

$3\text{--}4\text{ cm}^{-1}$. This can be increased to $\sim 20\text{ cm}^{-1}$ by varying the temperature of the QCL chip. Such a laser has the tremendous advantage of being very compact and rugged making it very useful for monitoring of a specific trace gas with resolved rotational structure. Depending upon what other gases are present, which might absorb in the same region, such a DFB-QCL may or may not be useful for monitoring a gas with a congested rotational spectrum by laser spectroscopy. With a limited tuning range, it is difficult to scan far enough to ascertain anything about the band profile of a congested band.

The spectral width of the QCL optical gain profile is usually significantly broader than 20 cm^{-1} and therefore QCLs can provide in fact a much broader wavelength tuning range. Recent advances have resulted in very broad gain profiles. The bound-to-continuum QC laser design first proposed by Blaser et al. [23] and the heterogeneous QC structure first demonstrated by C. Gmachl et al. as a super-continuum QCL [24], are the most promising structures in terms of broadband emission, and have been further developed for wide single mode frequency tuning spectroscopic applications by Maulini et al. [25]. A luminescence spectrum of 297 cm^{-1} FWHM at room temperature was observed for $\lambda \approx 10\text{ }\mu\text{m}$ QCL devices employing bound-to-continuum transitions [26], while even broader gain profiles with FWHM of $\sim 350\text{ cm}^{-1}$ were achieved in [25] using both concepts mentioned above by incorporating two bound-to-continuum designs emitting at 8.4 and $9.6\text{ }\mu\text{m}$.

To take advantage of the broadband gain of such QCLs, an external cavity (EC) configuration can be used to obtain a single mode operation at any wavelength within the laser gain profile [27, 28]. A widely tunable QC laser spectrometer implementing a novel EC-QCL architecture for high resolution spectroscopic applications and multi species trace-gas detection was recently demonstrated with a thermoelectrically cooled Fabry-Pérot gain medium operating in a continuous wave mode at $\lambda \sim 5.28\text{ }\mu\text{m}$. The instrument depicted in Fig. 2 employs a piezo-activated cavity mode tracking system for mode-hop free operation. The mode-tracking system provides independent control of the EC length, diffraction grating angle and laser current. The QCL gain medium allowed a coarse laser frequency tuning range of $\sim 155\text{ cm}^{-1}$ (see Fig. 3) and a high resolution (better than 0.001 cm^{-1}) continuous mode-hop free fine tuning within a range of up to 2 cm^{-1} with a maximum available optical power of $\sim 11\text{ mW}$.

Wide wavelength tunability around $\lambda = 5.28\text{ }\mu\text{m}$ allows accessing of most of the absorption lines within the fundamental vibrational band of NO as shown in the HITRAN simulation presented in Fig. 4a. A narrow laser linewidth of $< 30\text{ MHz}$, which allowed resolving spectral features separated by $\sim 0.01\text{ cm}^{-1}$, makes the EC-QCL an excellent light source suitable for high resolution spectroscopic applications and multiple species trace-gas detection (see measurements performed for a NO gas sample at both atmospheric and a reduced pressure of 10 Torr shown in Fig. 4b). The flexibility of this arrangement makes it possible to use it with any QCL gain media without the need of an embedded DFB structure and at any mid-infrared wavelength without changing the EC configuration.

More recently, the use of a MOCVD grown buried heterostructure Fabry-Pérot QCL gain medium operating at $\lambda = 8.6\text{ }\mu\text{m}$ in the above described EC-QCL sensor architecture resulted in considerably higher levels of optical output power (Fig. 5). The maximum single frequency output power obtained in the EC-QCL configuration was 50 mW , which represents a significant improvement compared with results obtained in [27] using a previous version of this system.

Until now we have considered only intersubband quantum cascade lasers (QCLs). The other form of quantum cascade laser is the interband cascade laser (ICL). These are

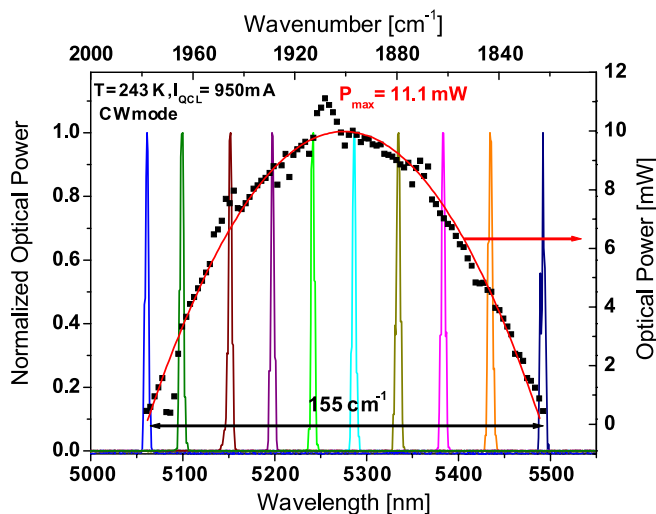


FIGURE 3 Wide wavelength tuning of a $5.3\text{ }\mu\text{m}$ EC-QCL

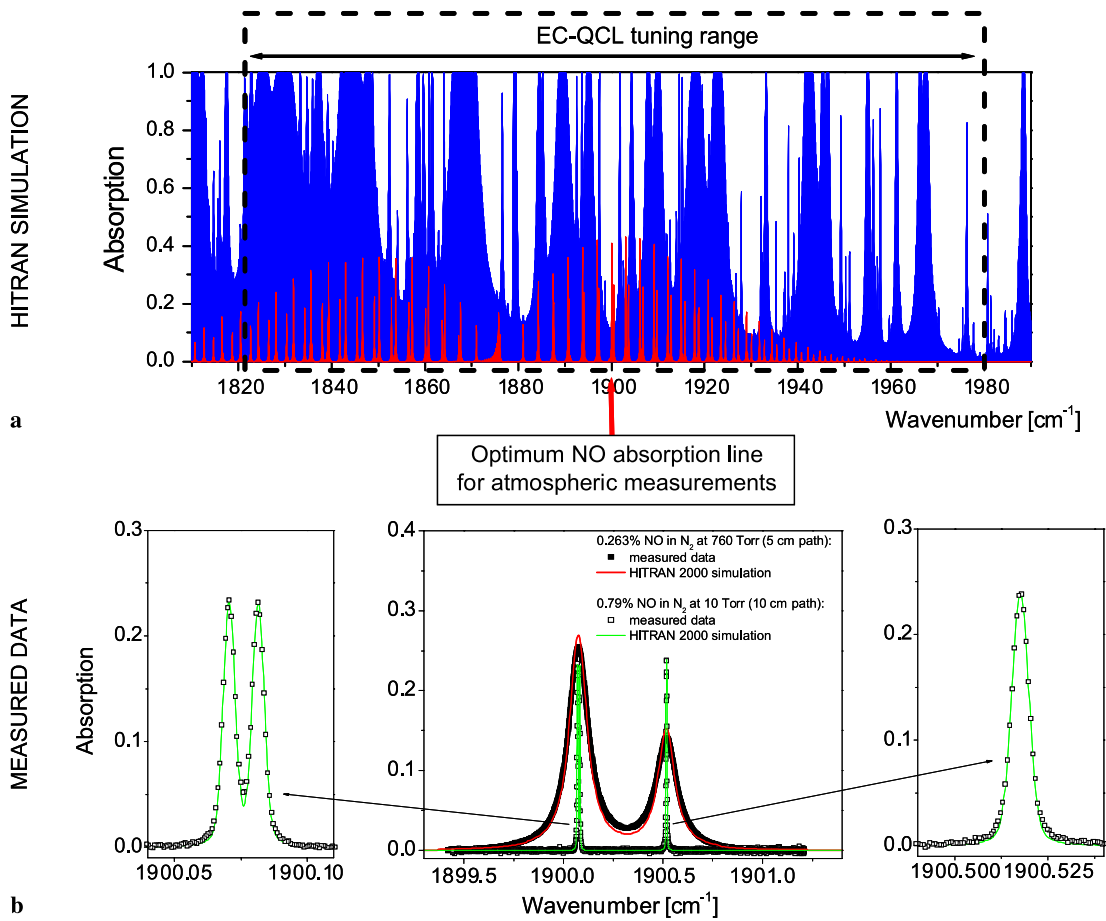


FIGURE 4 (a) Nitric oxide absorption spectra simulated for a 1 ppm NO mixture at atmospheric pressure and open path of 286 m (in red) shown together with an EC-QCL tunability range. Atmospheric absorption caused by H₂O (mixing ratio = 0.006) and CO₂ (mixing ratio = 380 ppm) is depicted in blue. (b) Spectral measurements performed for NO lines, which are optimal for atmospheric measurements (the narrow QCL linewidth allows a spectral resolution of $< 0.001 \text{ cm}^{-1}$)

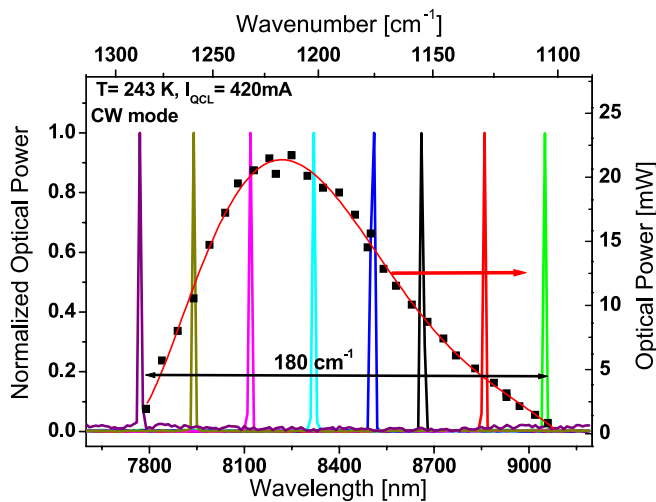


FIGURE 5 Wide wavelength tuning of an 8.4 μm EC-QCL

somewhat of a hybrid of a diode laser and a cascade laser. The lasing transition occurs when a conduction band electron confined in a quantum well of one material annihilates a quantum confined hole in the valence band of a different material emitting a photon. This is similar to a diode laser in that it is an interband transition, although with diode lasers

only a single material is typically involved. In a diode laser, each electron is used only once, while in an ICL an electron in the valence band well just tunnels out, and is raised in energy through a series of quantum wells until it possesses sufficient energy for the lasing transition process to be repeated. Thus the same electrical current is used repeatedly in a cascade process. Because they have band gap energy available, ICLs operate at shorter wavelengths than QCLs, typically in the 3–4 μm region. For various technical reasons, including that more types of semiconductor materials are employed, ICLs are more difficult to make, but they permit access to shorter wavelengths, as the short wavelength limit of QCLs is determined by the height of the well confinement barriers.

3 Fundamentals of trace gas sensing

3.1 Detection of power loss by absorption

Generally sensitivity and selectivity are the primary requirements for trace gas sensing. For small molecules with resolved rotational structure, selectivity is obtained by choosing an absorption line that is free of interference from other species that might be present in the sample. In the small molecule case, reducing the sample pressure sharpens the absorption line without reducing the peak absorption until the

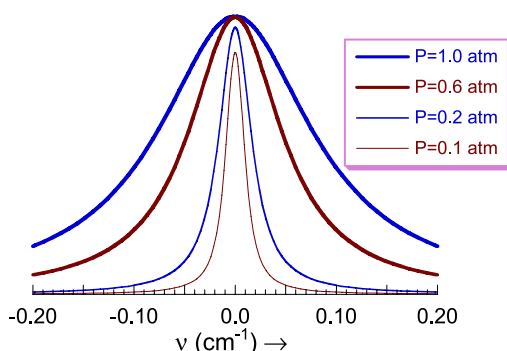


FIGURE 6 Pressure dependence of absorption

linewidth begins to approach the Doppler width, as is evident in Fig. 6. This sharpening of the absorption line significantly improves selectivity.

To obtain the best sensitivity one needs to choose a strong molecular absorption line, use a long pathlength, and have a means for distinguishing absorption from baseline variations and laser power fluctuations. The first requirement is best met by choosing a line of fundamental absorption bands as these tend to be stronger than overtone or combinations bands. An effective long pathlength can be obtained by using multipass cells or cavity enhancement techniques. For sharp absorption lines, noise associated with laser power fluctuations can be greatly reduced by averaging rapid scans over the line or by the similar technique of wavelength modulation. The final requirement to distinguish absorption from baseline variations is the most challenging. Every long pass arrangement exhibits accidental etalons, which typically have widths comparable to the absorption line width. In principle, these can be removed by evacuating the cell, replacing the sample with gas without the absorption (“zero air”) and then dividing the sample trace by this background trace. This approach assumes that these accidental etalons do not shift their pattern during the process of sample replacement, but this is often not the case.

Large molecules do not have resolved rotational structure, and a molecule does not have to be very large to be in this category. Molecules with four heavy atoms or low frequency vibrational modes typically are enough to cause congested spectra. Because there is no nearby baseline to compare with, the only way to detect absorption is by this process of pumping the sample out and replacing it with zero air. For very weak absorptions expected for trace concentrations this imposes severe limits on long term power stability of the laser source, the absence of low frequency laser noise, and baseline stability. Without a sharp rotational spectral component, the required long term power stability is typically ~ 1 in 10^4 . Furthermore in the mid-IR fingerprint region, where many gases absorb, there may be other gases contributing to a broad absorption putting selectivity in jeopardy. As we shall see, an advantage of photoacoustic spectroscopy is that the power stability and baseline stability requirements are reduced. However, any selectivity ambiguity in the molecules causing the absorption is not removed.

Turning to the practical matter of creating long effective pathlengths for absorption, some comparisons between the various means for doing this are needed. Open paths through

the atmosphere incur two problems: 1. There is no way to replace the sample with zero air making the baseline issue a serious problem and 2. there is no way to reduce the pressure in the path and atmospheric pressure linewidths (typically 0.1 cm^{-1}) are too large to be optimal. Obtaining a long pathlength by using a multipass cell suffers from neither of these problems; the only issue is that long pass multipass cells are intrinsically bulky. Cavity ringdown spectroscopy has been demonstrated to give excellent sensitivity, but requires very high quality mirrors, which are slowly becoming available in the mid-infrared. Optimum sensitivity requires a large spacing between the mirrors again making the trace gas sensor bulky. Off-axis intracavity absorption spectroscopy can provide long pathlengths in small volumes. Without further embellishments, its principal problem is mode noise arising from jumping between a welter of cavity modes. However, when the alignment of the cavity is such that the effective path traveled by the beam within the cavity before satisfying the reentrant condition is much longer than the laser coherence length (effective cavity FSR significantly smaller than the laser linewidth), or when combined with deliberately introduced vibration to move the mode structure rapidly and wavelength modulation to scramble them further, off-axis intracavity absorption spectroscopy has considerable promise for trace gas sensing especially as better mid-infrared mirrors become available.

3.2 Quartz-enhanced photoacoustic spectroscopy (QEPAS)

Photoacoustic spectroscopy (PAS) is based on the photoacoustic effect, in which acoustic waves are produced by the absorption of modulated radiation by target compound. By the use of specially designed cells, which are acoustically resonant at the modulation frequency and often contain an array of microphones, this is an effective method for sensitive trace gas detection. In contrast to other infrared absorption techniques, PAS is an indirect technique in which the effect on the absorbing medium and not the direct light attenuation is detected. Light absorption results in a transient temperature effect, which translates into pressure variations in the absorbing medium that can be detected with a sensitive microphone. PAS is ideally a background-free technique, since the signal is generated only by the absorbing gas. However, background signals can originate from nonselective absorption of the gas cell windows (coherent noise) and external acoustic (incoherent) noise. PAS signals are proportional to the pump laser power and therefore the maximum detection sensitivity that can be realized by means of the PAS technique is with high-power laser excitation. However, a sensitivity of 8 ppmv was demonstrated with only 2 mW of modulated diode laser power for CH_4 in its overtone region [29, 30]. The use of high power cw TEC QCL excitation in the fundamental absorption region gives results with much higher trace gas detection sensitivity.

A novel approach to photoacoustic detection of trace gases utilizing a quartz tuning fork (QTF) as a sharply resonant acoustic transducer was first reported in 2002 [31, 32]. The basic idea of quartz enhanced photoacoustic spectroscopy (QEPAS) is to invert the common PAS approach and accumu-

late the acoustic energy not in a gas-filled cell but in a sharply resonant acoustic transducer. A natural candidate for such a transducer is crystal quartz, because it is a low-loss piezoelectric material. A nearly optimum readily available quartz transducer can be found in the quartz tuning forks intended for use in electronic clocks and watches as frequency standards. QTFs typically resonate at 32 768 (2^{15}) Hz in clock circuits. A typical sensor architecture is depicted in Fig. 7a together with a picture of a QEPAS absorption detection module (ADM) consisting of a QTF equipped with a micro-resonator as shown in Fig. 7b. The laser radiation is focused between the prongs of the QTF and its wavelength is modulated at $f_m = f_0/2$ frequency or its intensity is modulated at $f_m = f_0$ frequency (where f_0 is the QTF resonant frequency) depending respectively on whether wavelength modulation or amplitude modulation of the laser is used. The acoustic wave at f_0 induced by absorption of the laser by the gas becomes the driving force to excite the symmetric fundamental mechanical vibration of the QTF prongs (i.e. the two QTF prongs move in opposite directions). The electrical signal produced by this piezo-electrically active mode of vibration is measured using lock-in detection at f_0 . Spectral data can be acquired by scanning the laser wavelength. To increase the effective interaction length between the radiation-induced sound and the QTF, a gas-filled acoustic resonator can be added somewhat similarly to the traditional PAS approach. Sound waves from distant acoustic sources tend to move the QTF prongs in the same direction, which results in zero net piezo-current thus making this element insensitive to such excitation.

Thus advantages of QEPAS compared to conventional resonant photoacoustic spectroscopy include QEPAS sensor immunity to environmental acoustic noise, a simple absorption detection module, and the capability to analyze small gas samples, down to 1 mm³ in volume. The pressure corresponding to optimum sensitivity depends upon the V to T energy conversion cross-section of the gas of interest. It was experimentally found that this optimum pressure for

fast-relaxing molecules with resolved optical transitions is ~ 50 Torr, which also ensures Doppler-limited spectral resolution. For slow relaxing gases such as NO or CO, this optimum pressure is higher and may give a broader linewidth than desirable for the best selectivity. The response speed of QEPAS is fundamentally limited by the resonance width of the QTF resonator, which at typical operating pressures is about 1 Hz. This constraint is of little concern for all but a very limited kind of application.

QEPAS sensor technology has already been demonstrated in trace gas measurements of 11 target analytes, including NH₃ [33], CO₂ [34, 35], N₂O [17], HCN [36], CO in propylene [37] and CH₂O [38]. A normalized noise equivalent absorption coefficient of $1.9 \times 10^{-9} \text{ cm}^{-1} \text{ W Hz}^{-1/2}$ was measured to date using QEPAS [39]. This figure of merit is comparable to the best conventional PA results. An experimental study of the long-term stability of a QEPAS-based NH₃ sensor showed that the sensor exhibits very low drift, which allows long term data averaging (> 3 h). This can provide a significant improvement of the signal to noise ratio in concentration measurements.

Recently Wojcik et al. [13] reported the performance of an amplitude modulated (AM) 8.4 μm QC laser based QEPAS sensor system that demonstrated the detection of broad band absorbing target species in the mid-infrared spectroscopic fingerprint region. Using a similar approach, we developed a QEPAS sensor employing an external cavity laser utilizing a MOCVD grown Fabry–Pérot QCL gain medium like the ones described in Sect. 2, targeting the unresolved absorption spectrum of C₂HF₅ (Freon 125) at $\lambda \sim 1150 \text{ cm}^{-1}$. The laser source exhibits single frequency tuning of 180 cm⁻¹. In this sensor a photoacoustic signal is generated by turning the laser on and off at the exact resonance frequency of the applied quartz tuning fork. The sensitivity of this sensor was determined both for a single point measurement as well as in a broadband wavelength scan using a calibration mixture of 15 ppm Freon-125A in dry nitrogen. With a laser

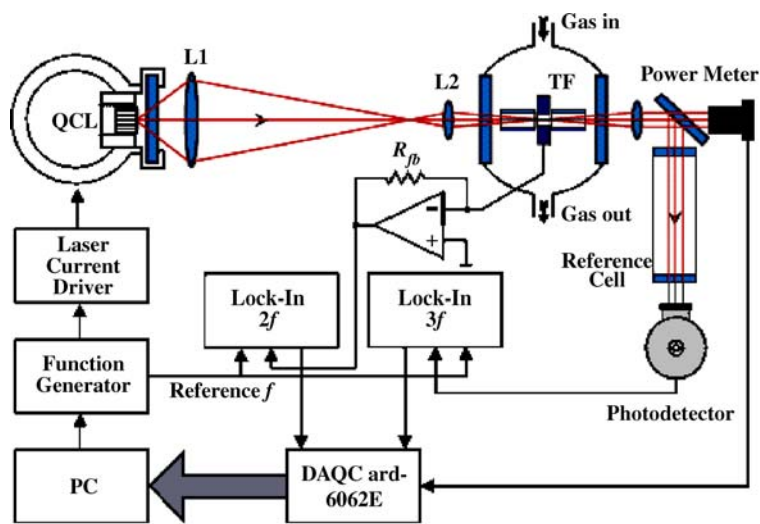


FIGURE 7 (a) Schematic of a QCL based QEPAS sensor platform showing a QTF and acoustic micro-resonator. (b) Picture of a QEPAS absorption detection module consisting of a QTF and micro-resonator

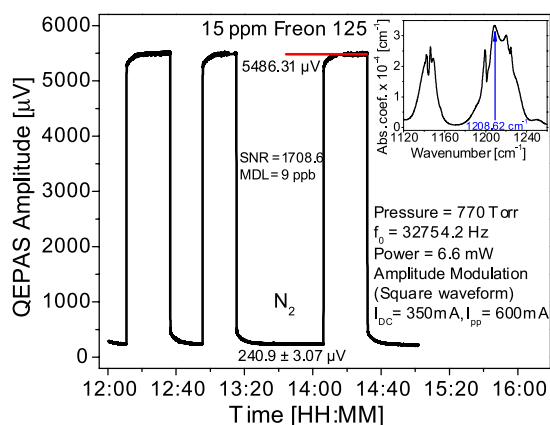


FIGURE 8 Freon 125A concentration measurement performed with a $8.6\ \mu\text{m}$ QCL based AM-QEPAS trace gas sensor system at the spectral location of a maximum absorption. The inset shows a spectral location of the laser frequency on the Freon 125 absorption spectrum

frequency set to $1208.62\ \text{cm}^{-1}$, which corresponds to the maximum absorption of Freon 125 in this spectral region, a continuous concentration measurement was performed. An example of an AM-QEPAS signal of the Freon 125 calibration mixture recorded between several subsequent zero gas flushes is shown in Fig. 8. A minimum detection limit (1σ) of $\sim 9\ \text{ppb}$ was calculated for these conditions based on the scatter of the background signal measurements. The power and measurement bandwidth normalized noise equivalent absorption coefficient (NNEA) of this sensor was determined to be $7.92 \times 10^{-9}\ \text{cm}^{-1}\ \text{W Hz}^{-1/2}$ for Freon 125. The applied cw TEC EC QC laser is able to provide $\sim 50\ \text{mW}$ of optical power. This translates into a minimum detection absorption coefficient limit for C_2HF_5 of $\sim 3.2 \times 10^{-7}\ \text{cm}^{-1}$ with 1 s averaging time.

AM detection of a broad band absorber at a single spectral point can only be performed for gas mixtures that do not contain species absorbing in the same spectral region. This limitation can be overcome by application of broadly tunable lasers, which can be tuned over a wide range of wavelengths

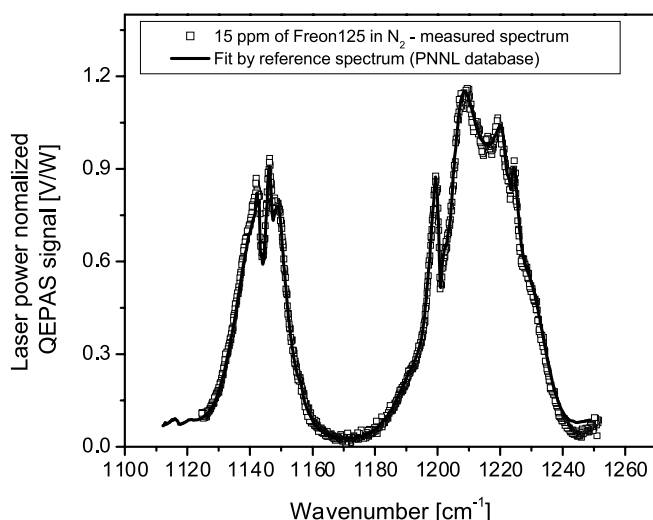


FIGURE 9 Photoacoustic spectrum of Freon 125 measured between 1125 and $1250\ \text{cm}^{-1}$ fitted by the reference spectrum from the spectral database

and allows measurement of a unique spectral envelope of the target unresolved absorption feature. EC-QCL seems to be an ideal tool for such application. Figure 9 depicts a spectrum of the same calibration mixture (15 ppm of Freon 125 in N_2), which was recorded with our EC-QCL based AM-QEPAS system. Excellent agreement of a measured spectrum with a spectrum obtained from a spectroscopic database (Pacific Northwest National Laboratory infrared spectral library) was observed. This in combination with appropriate data acquisition processing and analysis methods (see [40]) can allow concentration measurements with high molecular selectivity even in presence of spectrally interfering molecular species.

4 Trace gas sensing examples

4.1 NO using a high-finesse optical cavity

Detection of nitric oxide (NO) is important in many applications that include combustion diagnostics, [41], industrial emission and process monitoring [42] atmospheric research [43], and medical diagnostics [44, 45]. In recent years stricter regulatory limits for the maximum allowable concentrations of toxic pollutants in industrial exhaust gases are being imposed. This has triggered a need for sensors capable of real-time concentration monitoring of NO at parts per million (ppmv) levels to ensure regulatory compliance. An instrument suitable for direct in situ spectroscopic analysis of industrial exhaust gases must address specific environmental challenges including atmospheric analyte gas pressure, strong nonselective absorption by soot particles, high temperature, and absorption lines of different gas species [40]. Nelson et al.[46] reported measurements of nitric oxide in air with a detection limit of $< 1\ \text{ppb}$ using a thermoelectrically cooled quantum cascade laser operated in a pulsed mode at $5.26\ \mu\text{m}$ ($1897\ \text{cm}^{-1}$), with a line width of $\sim 0.01\ \text{cm}^{-1}$ (300 MHz), and coupled to a 210 m path length multiple-pass absorption cell at a reduced pressure (50 Torr). The sensitivity of the system is enhanced by normalizing pulse-to-pulse intensity variations with temporal gating on a single HgCdTe detector. A detection precision of $0.12\ \text{ppb Hz}^{-1/2}$ is achieved with a cryogenically-cooled detector. This detection precision corresponds to an absorbance precision of $1 \times 10^{-5}\ \text{Hz}^{-1/2}$ or an absorption coefficient per unit path length of $5 \times 10^{-10}\ \text{cm}^{-1}\ \text{Hz}^{-1/2}$.

Sensitive laser absorption spectroscopy often requires a long effective pathlength of the probing laser beam in media that are to be analyzed. Traditionally, this requirement is satisfied using an optical multipass cell. Such an approach can be difficult to implement in certain field applications, requiring compact gas sensor configurations. For example, a typical commercial 100 m pathlength multipass cell has a volume of 3.5 l. An alternative way to obtain a long optical path is to make the light bounce along the same path between two ultralow-loss dielectric mirrors forming a high finesse optical resonator. An effective optical pathlength of several kilometers can be obtained in a very small volume. The light leaking out of such an optical cavity can be used to characterize the absorption of the intracavity medium.

Presently a variety of techniques exist to perform high-sensitivity absorption spectroscopy in a high finesse optical cavity such as cavity ringdown spectroscopy (CRDS) [15]

or integrated cavity output spectroscopy (ICOS) [47–49]. In these techniques the coupling efficiency of the laser radiation into the resonant cavity is extremely critical and determines the amount of light which can be collected by a photodetector placed after the absorption cell. In an off-axis ICOS (OA-ICOS) arrangement, in which the optical system is aligned in such a way that the maximum number of longitudinal and transverse modes is excited within the cavity, the typical optical throughput of the cavity is on the order of $\leq T/2$ (where T is transmission of the cavity mirrors) [49]. In this case the system requires a very sensitive detector (usually cryogenically cooled) in order not to be limited by the detector noise floor. Therefore these techniques can also benefit from the increased laser power available from cw, high power QCLs, which results in substantial improvement of their detection sensitivities and/or allow use of less sensitive, but thermoelectrically cooled detectors, which is critical in field deployable gas sensor system.

A nitric oxide sensor based on a thermoelectrically cooled, cw DFB QCL laser operating at $\lambda = 5.45 \mu\text{m}$ (1835 cm^{-1}) and off-axis ICOS combined with a wavelength-modulation technique was developed to determine NO concentrations at the near 1 ppbv levels essential for a number of applications, such as in medical diagnostics (specifically in detecting NO in exhaled human breath) and environmental monitoring [19]. Exhaled nitric oxide (eNO) is an important biomarker in many respiratory diseases [50] and the exhaled NO levels have been extensively studied in asthma cases. These measurements may be clinically useful in other chronic respiratory conditions, such as chronic obstructive pulmonary disease (COPD), particularly if the NO contributions can be partitioned into alveolar and conducting airway regions. Exhaled NO levels generally range between 4 to 15 ppbv in healthy human subjects and 10–160 ppbv in subjects with untreated asthma when breath is collected at the standard 3 l/min, in accordance with the American Thoracic Society (ATS) recommendations [51–54].

The sensor shown in Fig. 10 employs a 50 cm-long high-finesse optical cavity that provides an effective path length of 700 m. A noise equivalent minimum detection limit of

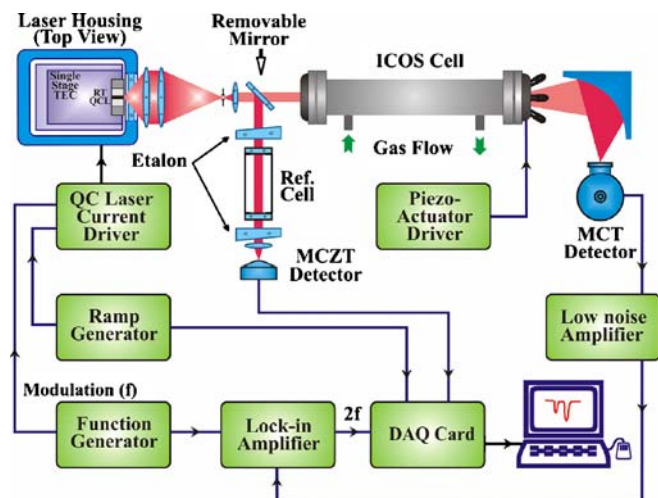


FIGURE 10 CW-TEC-DFB QCL laser based nitric oxide off axis-integrated cavity output spectroscopy

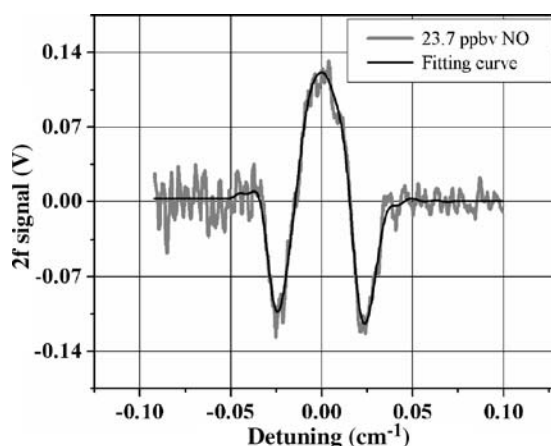


FIGURE 11 $2f$ OA-ICOS based NO absorption signal

0.7 ppbv with a 1 s observation time was achieved [16]. A wavelength modulated signal for a calibrated NO concentration of 23.7 ppbv was fitted using a general linear fit procedure [20] as shown in in Fig. 11.

Recently [55], a detection sensitivity of 0.03 ppbv was achieved with 30 s averaging time using a multipass gas cell with an optical path length of 210 m, corresponding to an absorption coefficient of $1.5 \times 10^{-10} \text{ cm}^{-1}$.

4.2 Air quality Measurements in Texas

Elevated concentration levels of ground-level ozone are the most serious air quality issue facing many urban areas today. Ground-level ozone is formed by the photochemical reactions of volatile organic compounds (VOCs) and nitrogen oxides (NO_x). Since ozone is not directly emitted from sources, but rather formed through atmospheric chemical reactions, air quality improvement plans must incorporate scientific understanding of how emissions, chemistry and transport convert precursor VOCs and NO_x into ozone. As a result, less progress has been made in attaining the health-based National Ambient Air Quality Standard (NAAQS) for ozone than for other pollutants regulated by the NAAQS that are directly emitted from sources (such as carbon monoxide or lead). In order to enable studies of this complex ozone chemistry, monitoring of several potential precursor molecules is required. Trace gas sensing methods that can provide in-situ, fast (~ 1 s response time) and sensitive (at ppb and lower levels) detection of molecules of interest can greatly aide in understanding the atmospheric chemistry of ozone precursors. All these requirements can be successfully addressed by laser spectroscopic trace-gas detection.

In the Greater Houston area, where emissions from high concentrations of petrochemical industrial sources combine with emissions from more traditional urban sources, the NAAQS for ozone is violated on roughly 45 days every year. Recently, emissions of VOCs from industrial sources have become the focus of air quality improvement plans in Houston, which are designed to reduce ambient ozone levels. Using aircraft sampling platforms and collecting whole air samples in evacuated stainless steel canisters which were then returned to a laboratory for analysis by gas chromatography (GC), quantification of VOCs from industrial sources indicated sig-

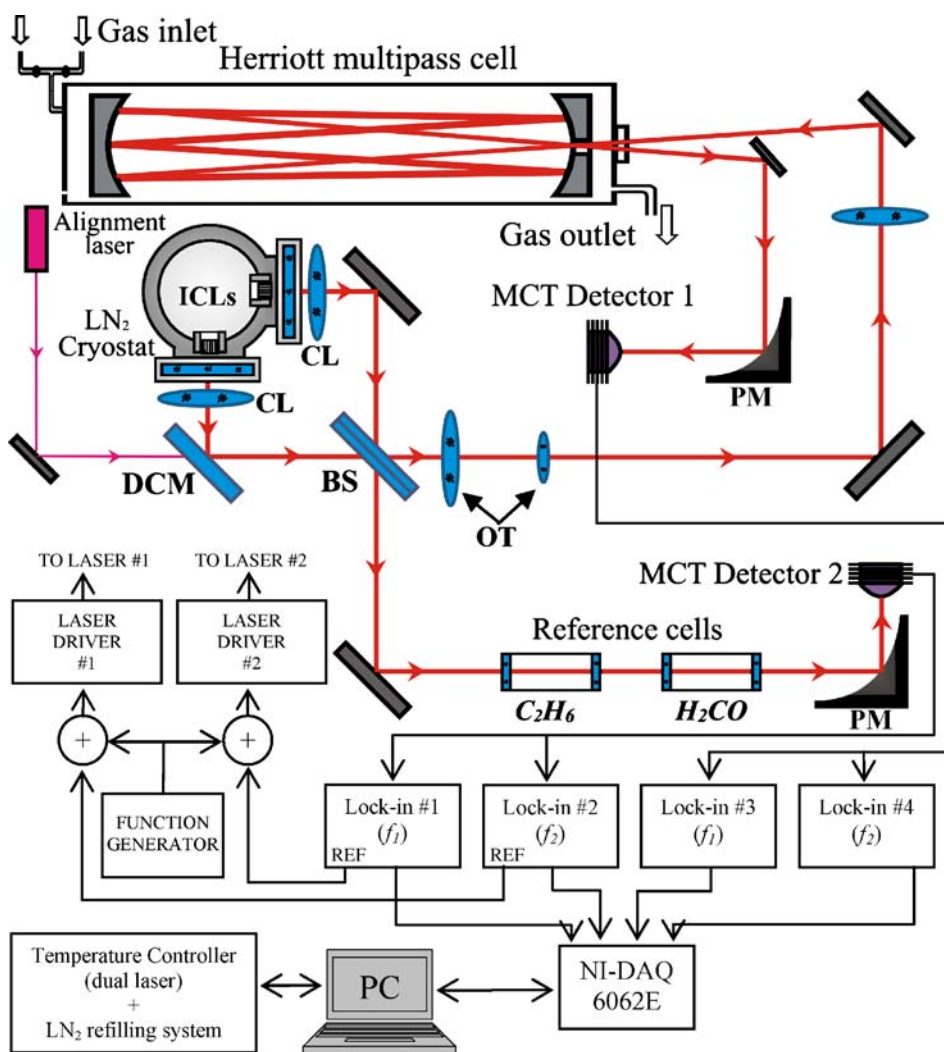


FIGURE 12 Schematic configuration of a dual ICL based trace gas sensor. ICL – interband cascade laser chip; DCM – dichroic mirror, BS – pellicle beam splitter, MCT – mercury-cadmium-telluride photodetector, CL – collimating lens; PM – off-axis parabolic mirror, OT – optical telescope, NI-DAQ – National Instruments data acquisition card

nificantly higher concentrations than expected [56, 57]. Using this type of data and models of atmospheric dispersion, it has been estimated that the emissions for VOCs from industrial sources in Houston exceed previously estimated emissions by a factor of 5–10. As a result, the uncertainty in the emission inventory for VOCs is a major concern for air quality improvement plans in Houston.

Hence, two of the most important trace gases to monitor for their ozone formation potential in Houston are ethylene (C₂H₄) and formaldehyde (H₂CO). Ethylene rapidly undergoes chemical oxidation leading to the formation of both ground-level ozone and also formaldehyde. Rapid quantification of these two gases (formaldehyde and ethylene) simultaneously leads to an improved understanding of the chemistry of ozone formation.

The sensor architecture is schematically shown in Fig. 12. It is considerably more complex than most because two lasers are being employed to simultaneously monitor two gases ethane and formaldehyde. The system uses ICL lasers, which currently require cryogenic cooling; thus, the two lasers are mounted in an LN₂ dewar. The dewar is equipped with two separately temperature-controlled cold fingers, which allows the use of two lasers with different operating temperatures. With the use of dewars and a large multipass cell, portability is be-

ing sacrificed for greater sensitivity and dual gas monitoring, but the instrument can easily be transported.

Figure 12 depicts the two ICL lasers that are collinearly propagated through the multipass cell to a single detector with the signals from each laser being separated by wavelength modulation of the lasers at different modulation frequen-

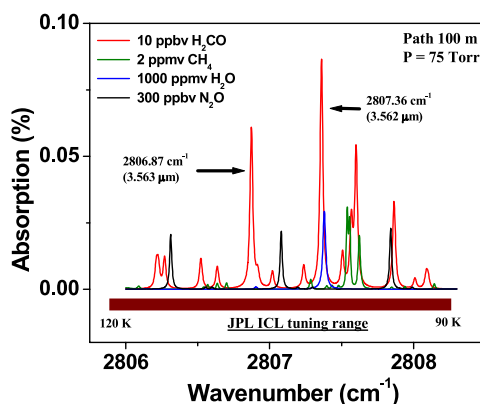


FIGURE 13 Simulated absorption spectrum of 10 ppbv H₂CO near 3.56 μm showing interferences including H₂O (1000 ppm), CH₄ (2 ppm) and N₂O (300 ppbv) at 75 Torr and with a 100 m effective optical path length

cies [58]. Indeed more than two channels can be introduced on one sensor platform without the need for increasing the number of photodetectors, and without the need for individual laser beam paths for each channel [59, 60]. However for concentration measurements, analytical or numerical simulation of $2f$ WMS spectra requires a significantly more complex data analysis that takes into account such parameters as absorption line shape, optical power, laser wavelength modulation depth, calibration of the wavelength scan, residual mod-

ulation of the laser power, and detector response. Although precise modeling of the $2f$ spectra is theoretically feasible, in practice the $2f$ WMS based trace gas sensors are calibrated using reference calibration gas mixtures [61]. More details of the system will be published [18].

As demonstrated in the laboratory tests the developed sensor in its present configuration is able to monitor H_2CO at ppb level, which is suitable for the atmospheric studies. Our initial goal was to configure the developed sensor to target both

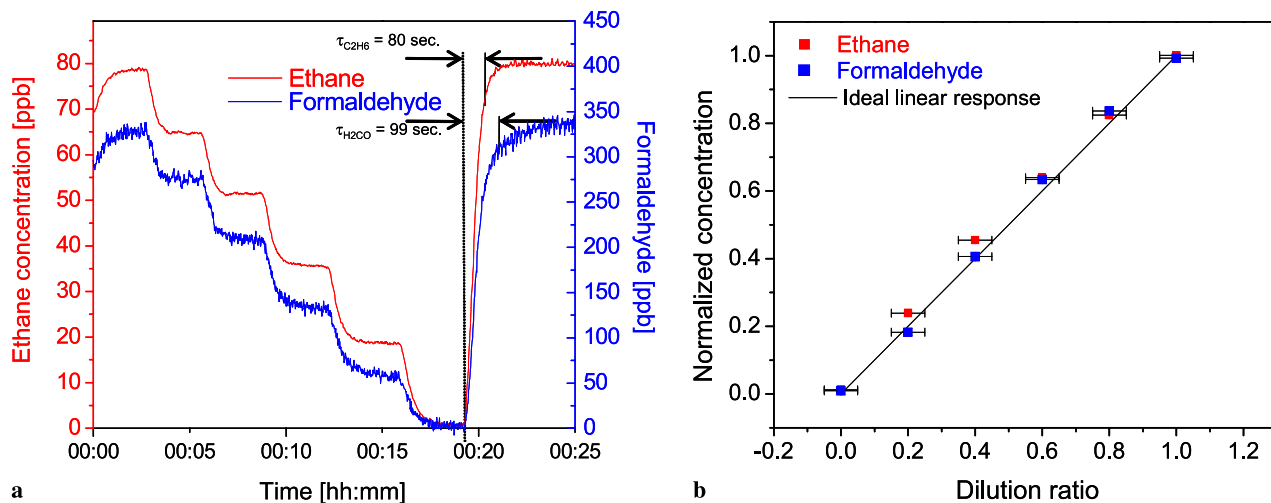


FIGURE 14 (a) Optical sensor response for two-channel operation targeting ethane ($3.33 \mu\text{m}$) and formaldehyde ($3.56 \mu\text{m}$). The initial gas mixture of $\sim 330 \text{ ppbv H}_2\text{CO}$ and $\sim 79 \text{ ppbv C}_2\text{H}_6$ is gradually diluted by pure N_2 . (b) Concentration measurements of ethane and formaldehyde normalized to their initial concentration level versus the dilution ratio (the error bars correspond to the precision of the dilution process)

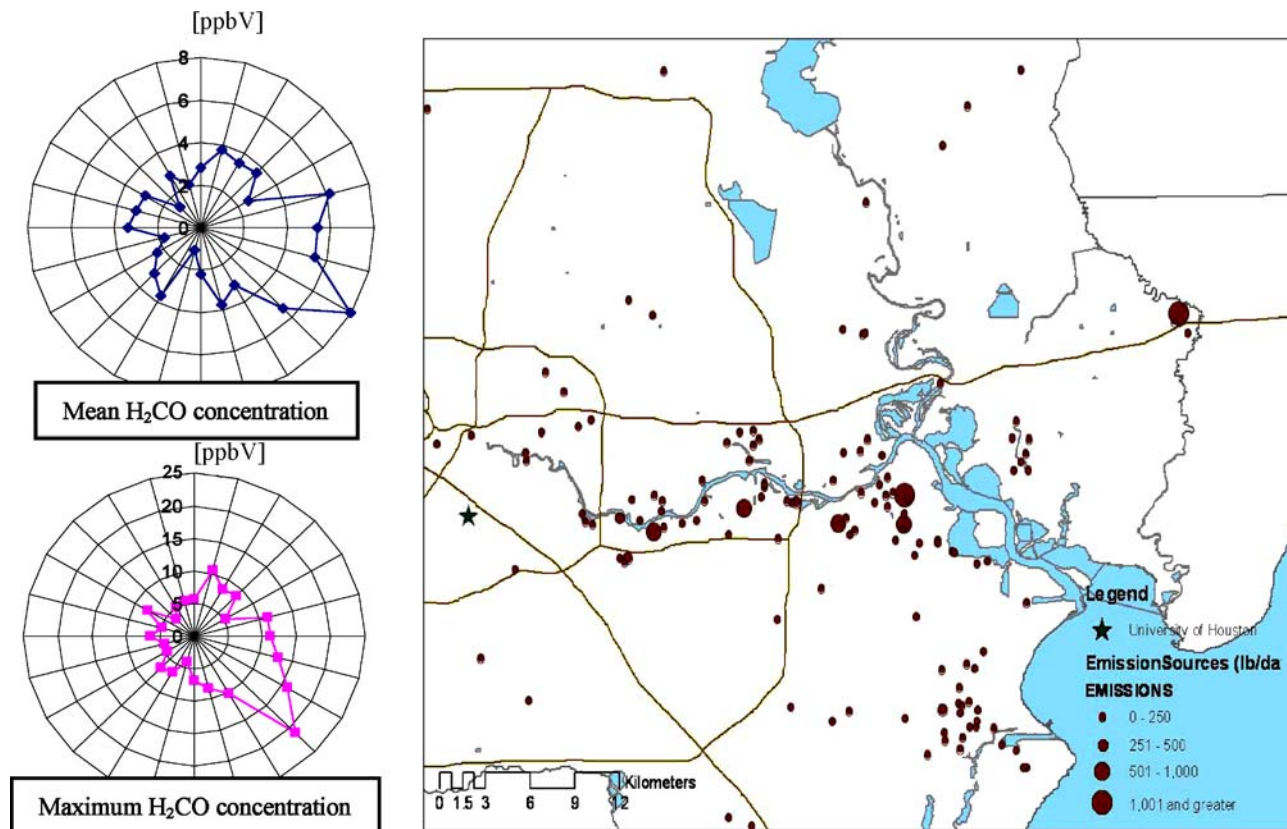


FIGURE 15 Mean level and maximum level of H_2CO concentration (ppbv) versus wind direction calculated using data from (data averaged within 15° angles). The map on the right shows the sampling site (marked with “*”) and major VOC sources in the Greater Houston area, Harris County [62]

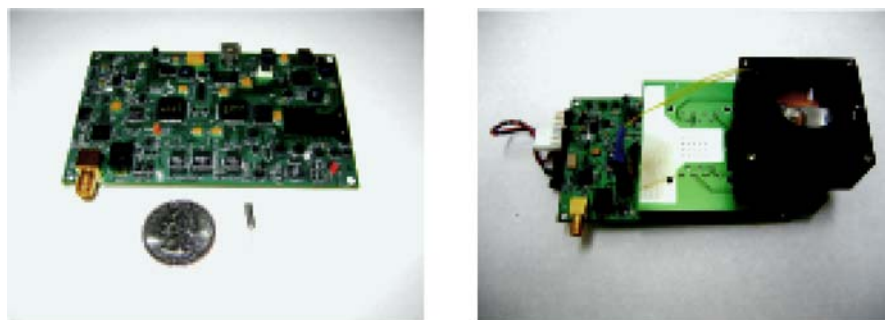


FIGURE 16 Miniature QEPAS CO₂ sensor operating at 2 μm

- Small Size
- Relatively Low Cost
- High Efficiency Switching Power Supplies
- PWM Peltier Cooler Driver
- 0.2W control system power consumption
- Similar detection limit to standard laboratory electronics
- Over 10³ sensitivity improvement @ 4.2 μm

molecules (H₂CO and C₂H₄) simultaneously, however at the time of our scheduled field test a suitable ICL targeting the ethylene was not available. The ICL based sensor described in this manuscript was deployed at the sampling site at the University of Houston main campus, which was one of the intensive monitoring sites in Houston during the TexAQS II campaign in August–September 2006. At this site a commercial formaldehyde sensor using Hantzsch reaction-based fluorometric detection was deployed by a research group from University of Houston, which provided an excellent opportunity for data intercomparison between an optical sensor and the traditional chemical technique.

The H₂CO measurements over the period from September 7–11, 2006 were correlated with the wind direction and the results are plotted in Fig. 13. Both the mean level and the maximum level of H₂CO concentration versus wind direction binned within 15° sections show clearly the industrial origin of H₂CO from the major VOC sources in Houston, Harris County (see the map in Fig. 15 for reference) [62]. Most of the time the maximum formaldehyde concentrations are seen when the wind comes from the direction of the petrochemical industry along the ship channel and Galveston Bay. The maximum concentration seems to be coming from the southeast, which is more in the direction of Texas City and Freeport and the industry located there.

5 Conclusions and future of chemical trace gas sensing

Compact, sensitive, and selective gas sensors based on quantum cascade lasers have been demonstrated to be effective in numerous real world applications. These now include such diverse fields as environmental monitoring (e.g. CO, CO₂, CH₄ and H₂CO are important carbon gases in global warming and ozone depletion studies), industrial emission measurements (e.g. fence line perimeter monitoring in the petrochemical industry, combustion sites, waste incinerators, gas well monitoring, gas pipeline and compressor sta-

tion safety), urban (e.g. automobile traffic, power generation) and rural emissions (e.g. horticultural greenhouses, fruit storage and rice agro-ecosystems), chemical analysis and process control for manufacturing processes (e.g. semiconductor, pharmaceutical, food), medical diagnostics that involves the detection and monitoring of biomarkers (e.g. NO, CO, CO₂, NH₃, C₂H₆ and CS₂), toxic gases and explosives relevant to law enforcement and public safety, as well as spacecraft habitat air-quality and planetary atmospheric science (e.g. planetary gases such as H₂O, CH₄, CO, CO₂ and C₂H₂).

With the development of efficient mid-infrared lasers [63–65] we envision the significant reduction of the size and cost of QCL trace gas monitors that will lead to the implementation of sensor networks [7, 66]. Some potential applications include monitor networks for the International Space Station or for detection of NH₃ in refrigerated food storage warehouses. The capability that networks can have of addressing applications that require both temporal and spatial resolution could lead to measurement of gas flow profiles such as the flow of methane from rice paddies. A prototype of a miniature a QEPAS CO₂ sensor operating at 2 μm is shown in Fig. 16.

ACKNOWLEDGEMENTS Financial support for the research performed by the current Rice Laser Science group (Y. Bakhrin, R.F. Curl, A. Kosterev, R. Lewicki, M. McCurdy, S. So, F.K. Tittel and G. Wysocki) was provided by the National Science Foundation via a sub-award from the Princeton University MIRTHERC, the National Aeronautics and Space Administration via awards from the Jet Propulsion Laboratory, Pasadena, CA and Johnson Space Center, Houston, TX, the Department of Energy via a sub-award from Aerodyne Research, the Savannah River National Laboratory, Aiken, SC, and the Robert Welch Foundation.

REFERENCES

- 1 F.K. Tittel, D. Richter, A. Fried, in *Solid state mid-infrared laser sources*, ed. by I.T. Sorokina, K.L. Vodopyanov (Springer, Berlin New York, 2003) Topics Appl. Phys., vol. 89, pp. 445–510
- 2 R.F. Curl, F.K. Tittel, *Ann. Rep. Prog. Chem. C* **98**, 219 (2002)
- 3 T. Yanagawa, H. Kanbara, O. Tadanaga, M. Asobe, H. Suzuki, J. Yumoto, *Appl. Phys. Lett.* **86**, 161 106 (2005)

- 4 D. Richter, P. Weibring, *Appl. Phys. B* **82**, 479 (2006)
- 5 P. Weibring, D. Richter, A. Fried, J.G. Walega, C. Dyroff, *Appl. Phys. B* **85**, 207 (2006)
- 6 A.A. Kosterev, F.K. Tittel, *IEEE J. Quantum Electron.* **QE-38**, 582 (2002)
- 7 S.G. So, G. Wysocki, J.P. Frantz, F.K. Tittel, *IEEE Sens. J.* **6**, 1057 (2006)
- 8 S. Borri, S. Bartalini, P. De Natale, M. Inguscio, C. Gmachl, F. Capasso, D.L. Sivco, A.Y. Cho, *Appl. Phys. B* **85**, 223 (2006)
- 9 S.C. Herndon, M.S. Zahniser, D.D. Nelson, J. Shorter, J.B. McManus, R. Jimenez, C. Warneke, J.A. de Gouw, *J. Geophys. Res. Atmosph.* **112**, 1003 (2007)
- 10 A. Lambrecht, T. Beyer, M. Braun, A. Peter, S. Hartwig, *Techn. Mess.* **71**, 311 (2004)
- 11 M.B. Pushkarsky, I.G. Dunayevskiy, M. Prasanna, A.G. Tsekoun, R. Go, C.K.N. Patel, *Proc. Nat. Acad. Sci.* **103**, 19630 (2006)
- 12 W.T. Rawlins, J.M. Hensley, D.M. Sonnenfroh, D.B. Oakes, M.G. Allen, *Appl. Opt.* **44**, 6635 (2005)
- 13 M.D. Wojcik, M.C. Phillips, B.D. Cannon, M.S. Taubman, *Appl. Phys. B* **85**, 307 (2006)
- 14 D. Weidmann, A.A. Kosterev, C. Roller, R.F. Curl, M.P. Fraser, F.K. Tittel, *Appl. Opt.* **43**, 3329 (2004)
- 15 A.A. Kosterev, A.L. Malinovsky, F.K. Tittel, C. Gmachl, F. Capasso, D.L. Sivco, J.N. Baillargeon, A.L. Hutchinson, A.Y. Cho, *Appl. Opt.* **40**, 5522 (2001)
- 16 Y.A. Bakhrkin, A.A. Kosterev, R.F. Curl, F.K. Tittel, D.A. Yarekha, L. Hvozdar, M. Giovannini, J. Faist, *Appl. Phys. B* **82**, 149 (2006)
- 17 A.A. Kosterev, Y.A. Bakhrkin, F.K. Tittel, *Appl. Phys. B* **80**, 133 (2005)
- 18 G. Wysocki, Y. Bakhrkin, S. So, F.K. Tittel, R.Q. Yang, M.P. Fraser, *Appl. Opt.* **46**, 8202 (2007)
- 19 M.R. McCurdy, Y.A. Bakhrkin, F.K. Tittel, *Appl. Phys. B* **85**, 445 (2006)
- 20 A.A. Kosterev, R.F. Curl, F.K. Tittel, R. Kohler, C. Gmachl, F. Capasso, D.L. Sivco, A.Y. Cho, *Appl. Opt.* **41**, 573 (2002)
- 21 A.A. Kosterev, Y.A. Bakhrkin, F.K. Tittel, S. Blaser, Y. Bonetti, L. Hvozdar, *Appl. Phys. B* **78**, 673 (2004)
- 22 <http://www.ece.rice.edu/lasersci/detectio.html>
- 23 S. Blaser, D. Yarekha, L. Hvozdar, Y. Bonetti, A. Muller, M. Giovannini, J. Faist, *Appl. Phys. Lett.* **86**, 41109 (2005)
- 24 C. Gmachl, D.L. Sivco, R. Colombelli, F. Capasso, A.Y. Cho, *Nature* **415**, 883 (2002)
- 25 R. Maulini, A. Mohan, M. Giovannini, J. Faist, E. Gini, *Appl. Phys. Lett.* **88**, 201113 (2006)
- 26 R. Maulini, M. Beck, J. Faist, E. Gini, *Appl. Phys. Lett.* **84**, 1659 (2004)
- 27 G. Wysocki, R.F. Curl, F.K. Tittel, R. Maulini, J.M. Bulliard, J. Faist, *Appl. Phys. B* **81**, 769 (2005)
- 28 C. Peng, G. Luo, H.Q. Le, *Appl. Opt.* **42**, 4877 (2003)
- 29 G.C. Liang, H.-H. Liu, A.H. Kung, A. Mohacsi, A. Miklos, P. Hess, *J. Phys. Chem. A* **104**, 10179 (2000)
- 30 M. Gomes da Silva, A. Miklos, A. Falkenroth, P. Hess, *Appl. Phys. B* **82**, 329 (2006)
- 31 A.A. Kosterev, Y.A. Bakhrkin, R.F. Curl, F.K. Tittel, *Opt. Lett.* **27**, 1902 (2002)
- 32 A.A. Kosterev, F.K. Tittel, D. Serebryakov, A. Malinovsky, A. Morozov, *Rev. Sci. Instrum.* **76**, 043105 (2005)
- 33 A.A. Kosterev, F.K. Tittel, *Appl. Opt.* **43**, 6213 (2004)
- 34 G. Wysocki, A.A. Kosterev, F.K. Tittel, *Appl. Phys. B* **85**, 301 (2006)
- 35 D. Weidmann, A.A. Kosterev, F.K. Tittel, N. Ryan, D. McDonald, *Opt. Lett.* **29**, 1837 (2004)
- 36 A.A. Kosterev, T.S. Mosely, F.K. Tittel, *Appl. Phys. B* **85**, 295 (2006)
- 37 A.A. Kosterev, Y.A. Bakhrkin, F.K. Tittel, S. Blaser, Y. Bonetti, L. Hvozdar, *Appl. Phys. B* **78**, 673 (2004)
- 38 M. Horstjann, Y.A. Bakhrkin, A.A. Kosterev, R.F. Curl, F.K. Tittel, *Appl. Phys. B* **79**, 799 (2004)
- 39 A. Kosterev, F.K. Tittel, T.S. Knittel, A. Cowie, J.D. Tate, Trace Humidity Sensor based on Quartz-Enhanced Photoacoustic Spectroscopy, *Laser Appl. to Chem. Security and Environ. Analysis Conf., Incline Village, NV, February 5–9 (2006)*
- 40 G. Wysocki, A.A. Kosterev, F.K. Tittel, *Appl. Phys. B* **80**, 617 (2005)
- 41 S. Wehe, M. Allen, X. Liu, J. Jeffries, R. Hanson, NO and CO absorption measurements with a MidIR quantum cascade laser for engine exhaust applications, *Proc. 41st Aerospace Sciences Meeting, 6–9 January (2003)*, Reno, Nevada, AIAA 2003-588
- 42 G.R. Price, K.K. Botros, G.M. Goldin, *J. Eng. Gas Turb. Power* **124**, 276 (2002)
- 43 C. Stroud, S. Madronich, E. Atlas, B. Ridley, F. Flocke, A. Weinheimer, B. Talbot, A. Fried, B. Wert, R. Shetter, B. Lefer, M. Coffey, B. Heikes, D. Blake, *Atmosph. Environ.* **37**, 3351 (2003)
- 44 P.E. Silkoff, M. Caramori, L. Tremblay, P. McClean, C. Chaparro, S. Kesten, M. Hutcheon, A.S. Slutsky, N. Zamel, S. Keshavjee, *Am. J. Resp. Crit. Care* **157**, 1822 (1998)
- 45 S.A. Kharitonov, P.J. Barnes, *Am. J. Resp. Crit. Care* **163**, 1693 (2001)
- 46 D.D. Nelson, J.H. Shorter, J.B. McManus, M.S. Zahniser, *Appl. Phys. B* **75**, 343 (2002)
- 47 B.A. Paldus, A.A. Kachanov, *Can. J. Phys.* **83**, 975 (2005)
- 48 Y.A. Bakhrkin, A.A. Kosterev, C. Roller, R.F. Curl, F.K. Tittel, *Appl. Opt.* **43**, 2257 (2004)
- 49 J. Paul, L. Lapson, J. Anderson, *Appl. Opt.* **40**, 4904 (2001)
- 50 K. Namjou, C.B. Roller, T.E. Reich, J.D. Jeffers, G.L. McMillen, P.J. McCann, M.A. Camp, *Appl. Phys. B* **85**, 427 (2006)
- 51 TS/ERS Recommendations for Standardized Procedures for the Online and Offline Measurement of Exhaled Lower Respiratory Nitric Oxide and Nasal Nitric Oxide. *Am. J. Resp. Crit. Care* **171**, 912 (2005)
- 52 T.H. Risby, S.F. Solga, *Appl. Phys. B* **85**, 421 (2006)
- 53 M. McCurdy, Y. Bakhrkin, G. Wysocki, F.K. Tittel, *J. Biomed. Opt.* **12**, 034034-1 (2007)
- 54 M. McCurdy, Y. Bakhrkin, G. Wysocki, F. K Tittel, *J. Breath Res.* **1**, 014001 (2007)
- 55 D.D. Nelson, J.B. McManus, S.C. Herndon, J. Shorter, M.S. Zahniser, S. Blaser, L. Hvozdar, A. Mueller, M. Giovannini, J. Faist, *Opt. Lett.* **21**, 2012 (2006)
- 56 L.I. Kleinman, P.H. Daum, D. Imre, Y.N. Lee, J.L. Nunnermacker, S.R. Springston, J. Weinstein-Lloyd, J. Rudolph, *Geophys. Res. Lett.* **29**, 1467 (2002)
- 57 T.B. Ryerson, M. Trainer, W.M. Angevine, C.A. Brock, R.W. Dissly, F.C. Fehsenfeld, G.J. Frost, P.D. Goldan, J.S. Holloway, G. Hubler, R.O. Jakoubek, W.C. Kuster, J.A. Neuman, D.K. Nicks, D.D. Parrish, J.M. Roberts, D.T. Sueper, *J. Geophys. Res.* **108**, 4249 (2003)
- 58 D.B. Oh, M.E. Paige, D.S. Bomse, *Appl. Opt.* **37**, 2499 (1998)
- 59 Y.Q. Li, K.L. Demerjian, M.S. Zahniser, D.D. Nelson, J.B. McManus, S.C. Herndon, *J. Geophys. Res.* **109**, D16S08 (2004)
- 60 R. Jimenez, S. Herndon, J.H. Shorter, D.D. Nelson, J.B. McManus, M.S. Zahniser, *Proc. SPIE Int. Soc. Opt. Eng.* **5738**, 318 (2005)
- 61 A. Fried, J.R. Drummond, B. Henry, J. Fox, *Appl. Opt.* **30**, 1916 (1991)
- 62 Texas Commission on Environmental Quality, Point Source Emission Inventory Database, provided by TCEQ Technical Analysis Division, Austin, TX (2006)
- 63 A. Tsekoun, R. Go, M. Pushkarsky, M. Razeghi, C.K.N. Patel, *Proc. Nat. Acad. Sci.* **103**, 4831 (2006)
- 64 A. Wittmann, M. Giovannini, J. Faist, L. Hvozdar, S. Blaser, D. Hofstetter, E. Gini, *Appl. Phys. Lett.* **89**, 141116 (2006)
- 65 J. Faist, *Appl. Phys. Lett.* **90**, 253512 (2007)
- 66 S. So, F. Koushanfar, A. Kosterev, F. Tittel, LaserSPEcks: Laser Spectroscopic trace gas sensor networks – sensor integration and applications, *Proc. Info. Process. in Sensor Networks (IPSN-SPOTS)*, Cambridge, MA, April 24–28 (2007)